Frontiers of Optoelectronics (2022) 15:41
https://doi.org/10.1007/s12200-022-00041-4

Frontiers of Optoelectronics

RESEARCH ARTICLE

Van der Waals epitaxial growth and optoelectronics of a vertical MoS_2/WSe_2 p–n junction

Yu Xiao[1] · Junyu Qu[1] · Ziyu Luo[1] · Ying Chen[1] · Xin Yang[1] · Danliang Zhang[2] · Honglai Li[1] · Biyuan Zheng[1] · Jiali Yi[1] · Rong Wu[1] · Wenxia You[1] · Bo Liu[1] · Shula Chen[1] · Anlian Pan[1]

Received: 14 April 2022 / Accepted: 21 April 2022

Abstract
Two-dimensional (2D) transition metal dichalcogenides (TMDs) have attracted extensive attention due to their unique electronic and optical properties. In particular, TMDs can be flexibly combined to form diverse vertical van der Waals (vdWs) heterostructures without the limitation of lattice matching, which creates vast opportunities for fundamental investigation of novel optoelectronic applications. Here, we report an atomically thin vertical p–n junction WSe_2/MoS_2 produced by a chemical vapor deposition method. Transmission electron microscopy and steady-state photoluminescence experiments reveal its high quality and excellent optical properties. Back gate field effect transistor (FET) constructed using this p–n junction exhibits bipolar behaviors and a mobility of 9 $cm^2/(V{\cdot}s)$. In addition, the photodetector based on MoS_2/WSe_2 heterostructures displays outstanding optoelectronic properties ($R = 8$ A/W, $D^* = 2.93 \times 10^{11}$ Jones, on/off ratio of 10^4), which benefited from the built-in electric field across the interface. The direct growth of TMDs p–n vertical heterostructures may offer a novel platform for future optoelectronic applications.

Keywords MoS_2 · WSe_2 · Chemical vapor deposition (CVD) · Vertical heterostructure · Optoelectronic transistor

1 Introduction

In the past decades, two-dimensional (2D) transition metal dichalcogenides (TMDs) layered semiconductors have been considered as promising candidates for next-generation electronics and optoelectronics. This is due to their unique properties such as atomically thin thickness, and to their electronic, photonic, and mechanical properties [1–6]. Moreover, the heterostructures that are composed of various 2D layered TMDs materials have attracted more and more attention as a consequence of their diversified band alignments [5]. For example, type-I materials are usually used for light-emitting diodes [7], type-II have an important application in photovoltaic devices [8, 9], and type-III are widely used in the tunneling field effect transistors [10]. Until now, there have been diverse ways to synthesize the heterostructures, including mechanical stacking, the solution method, and chemical vapor deposition (CVD) [12–14], in which the CVD approach can easily synthesize materials with high production yield and large area. Many van der Waals heterostructures have been successfully composed by the CVD method and can be used in integrated optoelectronic applications [15–17]. For instance, Li et al. reported high-performance optoelectronic devices based on van der Waals vertical MoS_2/$MoSe_2$ heterostructures with enhanced photoresponsivity of 36 A/W and a remarkable detectivity of 4.8×10^{11} Jones [16]. Wu et al. demonstrated the vapor growth of WSe_2/WS_2 heterostructures with distinct nonlinear optical properties by controlling crystallographic alignments in the form of AA and AB stacking [15]. However, although there is demand for mass production of high-quality vertical p–n heterostructures for use in integrated devices,

✉ Shula Chen
shuch@hnu.edu.cn

✉ Anlian Pan
anlian.pan@hnu.edu.cn

[1] Key Laboratory for Micro-Nano Physics and Technology of Hunan Province, College of Materials Science and Engineering, Hunan University, Changsha 410082, China

[2] School of Materials Science and Engineering, Key Laboratory for Micro-Nano Physics and Technology of Hunan Province, Hunan University, Changsha 410082, China

Published online: 11 October 2022

there are still few reports on them because synthesizing the non-alloyed heterojunctions with sharp interface by CVD method is difficult. Most of the devices developed so far are based on single-material [18–21], but their performance is limited by defects and small light absorption cross-sections [21, 22]. Therefore, the controllable synthesis of vertical p–n heterostructures is very important for future integrated electronic and optoelectronic applications.

In this work, we report production of vertical MoS_2/WSe_2 p–n heterojunctions through a two-step CVD method and explore its application in photoelectric devices. The optical measurements and scanning transmission electron microscopy (STEM) demonstrate that the heterostructures are of high quality, without alloying. Electrical measurements exhibit considerable photon-electron conversion efficiency, photoresponsivity, detectivity, and stable light response. The study thus provides an alternative approach to design various TMDs heterostructures for future optoelectronic applications.

2 Experimental details

2.1 Synthesis of MoS_2/WSe_2 vertical heterostructures

The vertical MoS_2/WSe_2 heterostructures were synthesized by a two-step growth CVD approach. In the first step, MoS_2 template was synthetized using a salt-assisted method, Salt could reduce the evaporation temperature of MoO_3, thereby reducing the difficulties for production of MoS_2 with large-area. An alumina boat containing S powder was placed at upstream of a furnace. Then, another boat with mixed powder of NaCl and MoO_3 (99.99%, Alfa Aesar) was positioned at the central region of furnace, on top of which three pieces of SiO_2/Si substrates was placed for deposition. Before heating, the system was cleaned by pure Ar flow for 30 min at a rate of 80 standard cubic centimeters per minute (sccm). The furnace was heated to 810 ℃ within 30 min at 60 sccm, with Ar as the carrier gas, then maintained at that temperature for a further 10 min. Finally, the furnace naturally cooled down to room temperature. For the second step, to synthesize vertical WSe_2/MoS_2 heterostructures, a boat with as-grown MoS_2 templates was placed at downstream of furnace for subsequent deposition of WSe_2. The WSe_2 source powder (99.99%, Alfa Aesar) was put at the central heating area of the furnace. After the cleaning procedure as described above, the furnace was heated to 1020 ℃ within 30 min at 60 sccm and maintained at that temperature for 3 min. After the reaction, the furnace cooled down to room temperature naturally.

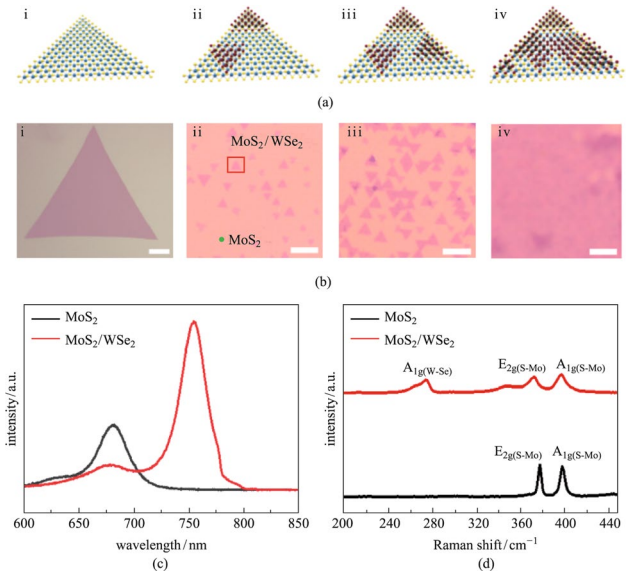

Fig. 1 Growth morphology and the optical characterizations of as-grown MoS_2/WSe_2 heterostructures. Schematic views of heterostructure growth ($\mathbf{a}_i$–$\mathbf{a}_{iv}$) and their corresponding optical images ($\mathbf{b}_i$–$\mathbf{b}_{iv}$). Scale bar: 20 μm. **c** PL spectra of monolayer MoS_2 and MoS_2/WSe_2 heterostructure. **d** Raman spectra of MoS_2 and MoS_2/WSe_2 heterostructure

2.2 Characterizations

The morphologies of heterostructures were characterized using an optical microscopy (Zeiss Axio Scope A1), an atomic force microscope (AFM, Bruker Multimode 8), and a scanning transmission electron microscope (JEM ARM200F). The optical measurements (Photoluminescence and Raman) were conducted using a confocal microscope (WITec, alpha-300) with a 532 nm laser focused by an objective.

2.3 Device fabrication and optoelectronic measurements

Standard e-beam lithography (EBL, Raith 150) and metal thermal evaporation were performed to fabricate the Au/Cr (10 nm/50 nm) electrodes on the as-grown heterostructures with a lift-off approach. The electric and optoelectronic properties of the heterostructures were measured in vacuum with Lake Shore Probe Station and Agilent B1500A semiconductor analyzer at room temperature.

3 Results and discussion

The MoS_2/WSe_2 heterostructures were grown by a two-step CVD method. Figure 1a shows a schematic diagram of the atomic growth model, and Fig. 1b exhibits a picture of the heterostructure under the optical microscope. The schematic

view and optical image of MoS_2 grown on SiO_2/Si substrate are shown in Figs. 1a_i and 1b_i (Additional file 1: Fig. S1 for detail) respectively. The lateral size of monolayer MoS_2 triangles ranged from 20 to 200 μm. The red square in Fig. 1b_{ii} indicates the small WSe_2 triangles that was grown on MoS_2 in the second step, and the area marked by the green spots is the underlying MoS_2. The evolution of morphology of WSe_2 on MoS_2 after 2, 4, and 6 min growth is shown in Figs. 1a_{ii}–a_{iv} and 1b_{ii}–b_{iv}, respectively, with the whole WSe_2 covered eventually. The optical image clearly indicated that WSe_2 on MoS_2 had only 0° and 60° stacking modes. Atomic force microscopy showed that MoS_2 and WSe_2 were both monolayers (Additional file 1: Fig. S2). Figure 1c shows the photoluminescence (PL) spectra of MoS_2 and MoS_2/WSe_2 heterostructures. The peaks at 680 and 755 nm correspond to the A excitons of MoS_2 and WSe_2, respectively. The PL intensity of MoS_2 becomes quenched in the heterostructure because of the charge transfer in the MoS_2/WSe_2 interface, with type-II band alignment, as shown in Fig. 4f. Figure 1d shows the Raman spectra of MoS_2 and MoS_2/WSe_2heterostructure. The peak positions of MoS_2 locate at 379 cm^{-1} ($E_{2g(S\text{-}Mo)}$) and 397 cm^{-1} ($A_{1g(S\text{-}Mo)}$), respectively, while that of the heterostructure locate at 270 cm^{-1} ($A_{1g(W\text{-}Se)}$), 372 cm^{-1} ($E_{2g(S\text{-}Mo)}$), and 400 cm^{-1} ($A_{1g(S\text{-}Mo)}$). PL and Raman results are consistent with MoS_2 and WSe_2 properties previously reported, proving the successful synthesis of MoS_2/WSe_2 heterostructure.

The MoS_2/WSe_2 heterostructure grown on SiO_2/Si was transferred to a copper net (see the supporting information for the detail transfer method), and then the microstructure and chemical composition of the MoS_2/WSe_2 heterostructure were analyzed by transmission electron microscopy (TEM). Figure 2a gives the low-resolution scanning transmission electron microscope (TEM) image of MoS_2/WSe_2 vertical heterostructure. The triangular area marked by green dash line is the bottom layer of MoS_2, and the red triangle is the heterojunction area. Figure 2b is the high-resolution transmission electron microscope (HRTEM) image of the bottom MoS_2, with a lattice spacing of 2.7 Å, corresponding to the (100) crystal plane of the 2H phase MoS_2. The inset is the selected area electron diffraction (SAED) pattern of MoS_2. The SAED of the MoS_2/WSe_2 heterostructure is shown in Fig. 2c. Two sets of regular hexagon diffraction pattern are displayed clearly. The polygonal diffraction patterns marked by green and red lines have a crystal plane spacing of 2.7 Å and red 2.8 Å, corresponding to MoS_2 and WSe_2 (100) crystal planes, respectively. Figure 2d shows the area at the interface of the heterostructure under the HRTEM. The right side is MoS_2, and the left side is the heterostructure. The atomic structure is clear, which proves that the high-quality MoS_2/WSe_2 vertical heterojunction with a clear interface was successfully synthesized. The TEM energy-dispersive X-ray photoelectron spectroscopy (EDS) of different regions

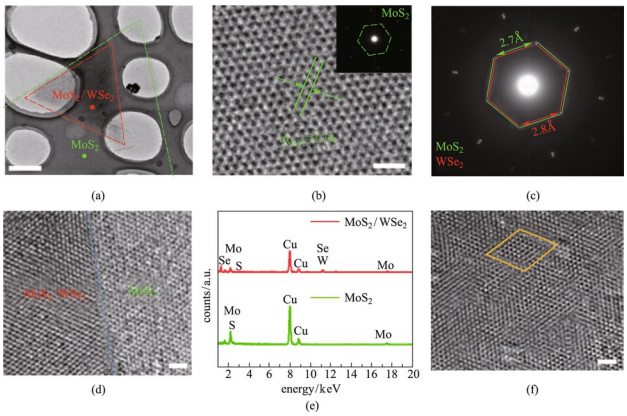

Fig. 2 High-resolution atomic characterizations of MoS_2/WSe_2 heterostructure. **a** Low-resolution TEM image of transferred MoS_2/WSe_2 heterostructure on a Cu grid. Scale bar: 1 μm. **b** HRTEM image of MoS_2. Scale bar: 1 nm. **c** SAED patterns of MoS_2/WSe_2 heterostructure. **d** Atomic resolution scanning TEM image of the heterostructure interface. Scale bar: 2 nm. **e** EDS spectra of the MoS_2/WSe_2 vertical heterostructure. **f** HRTEM image of heterostructure region. Scale bar: 2 nm

is shown in Fig. 2e. The red line shows several peaks for elements such as W, Se, Mo, S, and Cu (from the copper mesh), corresponding to the MoS_2/WSe_2 heterojunction. The green line only shows Mo, S, and Cu peaks, corresponding to the MoS_2. The results agrees with The X-ray photoelectron spectroscopy (XPS) measurement of the heterojunction given in Additional file 1: Fig. S3. Figure 2f is the HRTEM image in the heterojunction region, the moiré patterns can be clearly observed due to the interlayer coupling between MoS_2 and WSe_2. This observation further demonstrates the successful synthesis of the high-quality, well-defined MoS_2/WSe_2 heterostructure.

To further investigate the charge transport properties of the vertically stacked MoS_2/WSe_2 van der Waals heterostructures, back-gate field-effect transistors (FET) were fabricated based on MoS_2/WSe_2 p–n heterojunctions. Figure 3a displays the device structure in which Ti/Au electrodes are deposited on WSe_2, as the drain and source electrodes. The transport characteristic of the heterostructure device given in Fig. 3b shows ambipolar behavior, which is attributed to the p-type WSe_2 and the n-type MoS_2. Figure 3b shows that, when a negative gate voltage (V_g) is applied, the WSe_2 layer is turned on and the device exhibits p-type behavior. Conversely, when the MoS_2 layer is on state and the device shows n-type behavior while the gate voltage was positive. At the same time, the current increases when the drain-source voltage V_{ds} changes from 0.2 to 1 V. The diagram indicates that the threshold voltage is − 10 V, and the on/off ratio is 10^4. The mobility could be obtained using the expression $\mu = g_m L/(WC_0V_{ds})$, where g_m represents the transconductance, $L = 17.3$ μm and $W = 54.5$ μm are the length and the width of

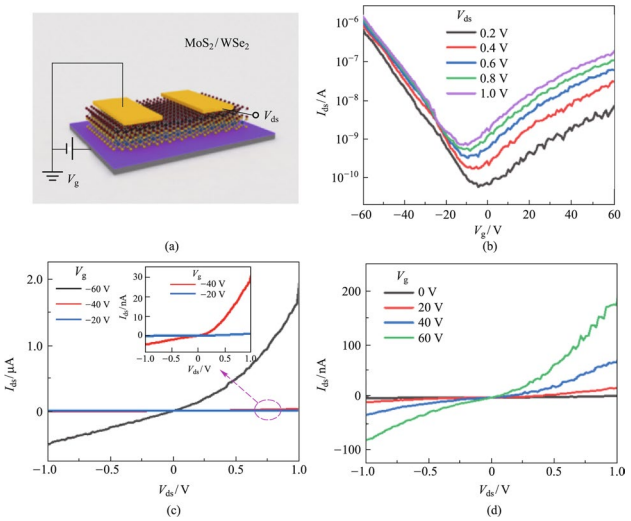

Fig. 3 Electronic characterization of MoS_2/WSe_2 heterostructure transistors. **a** Schematic configuration. **b** Transfer characteristic curves. **c**, **d** I_{ds}–V_{ds} output characteristics curves at various gate voltages ranging from − 60 to 60 V

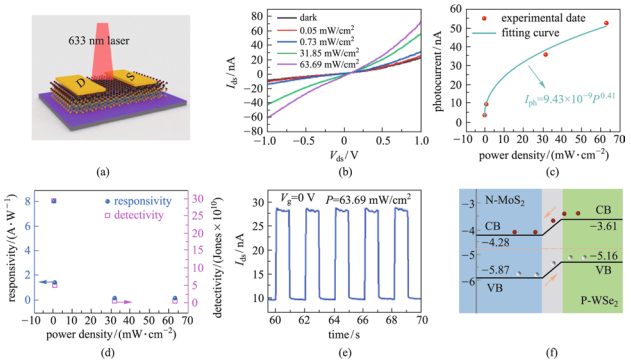

Fig. 4 Optoelectronic device performance of MoS_2/WSe_2 vertical heterostructure. **a** Schematic illustration of the device. **b** I_{ds}–V_{ds} curves across the heterojunction under 633 nm laser illumination with different incident powers. V_{ds} ranges from – 1 to 1 V. **c** Dependence of device photocurrent on illumination power densities. **d** Photoresponsivity and detectivity of the photodetector at various illumination power densities ranging from 0 to 63.69 mW/cm^2. **e** Photocurrent response of the device; the laser excitation is turned on and off by a chopper working at 1 Hz (V_{ds} = 1 V, V_g = 0 V, P = 63.69 mW/cm^2). **f** Band structures and the charge transfer process at the interface of the MoS_2/WSe_2 p–n heterojunction

the device, respectively. C_0 is the capacitance per unit area for the 280 nm thick SiO_2. Based on the data shown in Fig. 3b, the calculated mobility is 9 cm^2/(V·s). Figure 3c, d show the corresponding output characteristics of MoS_2/WSe_2 heterostructure. The inset in Fig. 3c is the enlarged view of the region marked by the red circle. The drain-source current I_{ds} decreases as the V_g varies from − 60 to − 20 V, and increases as V_g raises from 0 to 60 V. All the device measurements were conducted under vacuum at room temperature.

Benefiting from the large built-in electric field at the p–n heterojunction interface and the resulting high separation efficiency of photogenerated carriers, p–n heterostructures are widely used in optoelectronic applications. Under illumination of 633 nm laser light, the photovoltaic and photoresponse characteristics of the MoS_2/WSe_2 vertical heterostrutures were examined further. The photodetector based on MoS_2/WSe_2 vertical heterjunction is schematically illustrated in Fig. 4a, with drain-source voltage V_{ds} applied to the heterojunction device. Figure 4b shows the I_{ds}–V_{ds} curves at various illumination intensities ranging from 0 to 63.69 mW/cm^2 (V_g = 20 V). More electron–hole pairs are generated as the illumination intensity increases, resulting in a greater photocurrent. In Fig. 4c, the photocurrent intensities are evaluated at a gate bias of 20 V. Other photocurrent data under different gate voltages are shown in Additional file 1: Fig. S4a. The photocurrent intensity (I_{ph}) is defined as $I_{ph} = I_{light} - I_{dark}$, where I_{light} (I_{dark}) is current measured under light (dark state). The relation between I_{ph} and laser power density P can be expressed as $I_{ph} = aP^{\alpha}$. The fitted parameters of a and α obtained from Fig. 4c are 9.43×10^{-9} and 0.41, respectively. The responsivity (R) can be calculated using $R = I_{ph}/(PA)$, where A is the effective area of the device channel. The calculated responsivity of the device is up to 8 A/W (P = 0.05 mW/cm^2, V_{ds} = 1 V, device area of 943.85 μm^2), which is greater than that of monolayer MoS_2 and WSe_2 devices previously reported [24–26]. In addition, the value of R can reach up to 41 A/W at 60 V gate voltage (Additional file 1: Fig. S4b). To characterize the sensitivity of a photodetector, the device detectivity (D^*) is used. D^* can be calculated using the formula $D^* = RA^{1/2}/(2eI_{dark})^{1/2}$, where e is the electron charge, assuming D^* is primarily affected by the shot noise of the dark current [26, 27]. According to this formula, D^* can reach a maximum value of 2.93×10^{11} Jones as shown in Fig. 4d. Detectivity at various gate voltages can be found in Additional file 1: Fig. S4c. The photoresponse speed of the $MoS_2/MoSe_2$ heterostructure photodetector was investigated further by turning on and off the laser beam (633 nm, 63.69 mW/cm^2). Figure 4e displays exemplary photocurrent curves for the photodetector, showing excellent stability and reliability of on/off switching behavior (V_{ds} = 1 V, V_g = 0 V, P = 63.69 mW/cm^2). Figure 4f exhibits the band structure of the MoS_2/WSe_2. It is shown that a typical type-II heterostructure is formed. When the laser beam was focused on the heterojunction, the electrons in WSe_2 were transferred to MoS_2, whereas the holes in MoS_2 were transferred to WSe_2. This results in the photogating effect, wherein the charges modify the conductance of the WSe_2 channel. The high responsivity and the excellent reliability indicate that the designed MoS_2/WSe_2 p–n heterojunction may achieve ultrasensitive photodetection in the future.

4 Conclusions

In this work, we developed a controllable two-step growth method to prepare vertically stacked MoS_2/WSe_2 heterostructures. Furthermore, PL Spectroscopy, Raman spectroscopy, and HRTEM were used to characterize the obtained p–n heterojunctions. The results indicate that the samples are of high crystal quality. A p–n field effect transistor was fabricated based on the heterostructures. The bipolar behavior was observed and the device exhibited high carrier mobility of up to 9 $cm^2/(V{\cdot}s)$. Under the laser illumination, excellent photodetection properties was obtained with the photoresponsivity approaching 8 A/W and detectivity of 2.93×10^{11} Jones. Meanwhile, stable on/off photoswitching was also demonstrated. All the results show that the achieved MoS_2/WSe_2 p–n heterojunctions have great potential in integrated optoelectronic applications.

Supplementary Information The online version contains supplementary material available at https://doi.org/10.1007/s12200-022-00041-4.

Acknowledgements The authors are grateful to the National Natural Science Foundation of China (Grant Nos. 62090035, U19A2090, and 61905071), the Key Program of the Hunan Provincial Science and Technology Department (Nos. 2019XK2001 and 2020XK2001), and the International Science and Technology Innovation Cooperation Base of Hunan Province (No. 2018WK4004).

Author contributions YX, SLC, and ALP conceived the idea and participated in the data analysis. YX performed the material growth, optical characterization and drafted the manuscript. All authors read and approved the final manuscript.

Declarations

Competing interests The authors declare that they have no competing interests.

References

1. Zeng, H., Dai, J., Yao, W., Xiao, D., Cui, X.: Valley polarization in MoS^2 monolayers by optical pumping. Nat. Nanotechnol. **7**(8), 490–493 (2012)
2. Duan, X., Wang, C., Pan, A., Yu, R., Duan, X.: Two-dimensional transition metal dichalcogenides as atomically thin semiconductors: opportunities and challenges. Chem. Soc. Rev. **44**(24), 8859–8876 (2015)
3. Seyler, K.L., Schaibley, J.R., Gong, P., Rivera, P., Jones, A.M., Wu, S., Yan, J., Mandrus, D.G., Yao, W., Xu, X.: Electrical control of second-harmonic generation in a WSe_2 monolayer transistor. Nat. Nanotechnol. **10**(5), 407–411 (2015)
4. Li, H., Wang, X., Zhu, X., Duan, X., Pan, A.: Composition modulation in one-dimensional and two-dimensional chalcogenide semiconductor nanostructures. Chem. Soc. Rev. **47**(20), 7504–7521 (2018)
5. Zheng, W., Zheng, B., Yan, C., Liu, Y., Sun, X., Qi, Z., Yang, T., Jiang, Y., Huang, W., Fan, P., Jiang, F., Ji, W., Wang, X., Pan, A.: Direct vapor growth of 2D vertical heterostructures with tunable band alignments and interfacial charge transfer behaviors. Adv. Sci. **6**(7), 1802204 (2019)
6. Luo, Z., Zheng, W., Luo, N., Liu, B., Zheng, B., Yang, X., Liang, D., Qu, J., Liu, H., Chen, Y., Jiang, Y., Chen, S., Zou, X., Pan, A.: Photoluminescence lightening: extraordinary oxygen modulated dynamics in WS_2 monolayers. Nano. Lett. **22**(5), 2112–2119 (2022)
7. Lu, Z.H., Baribeau, J.M., Lockwood, D.J.: Quantum confinement and light emission in SiO_2/Si superlattices. Nature **378**(6554), 258–260 (1995)
8. Liu, H., Zhu, X., Sun, X., Zhu, C., Huang, W., Zhang, X., Zheng, B., Zou, Z., Luo, Z., Wang, X., Li, D., Pan, A.: Self-powered broadband photodetectors based on vertically stacked WSe_2/Bi_2Te_3 p–n heterojunctions. ACS Nano **13**(11), 13573–13580 (2019)
9. Yuan Y., Zhang, X., Liu, H., Yang, T., Zheng, W., Zheng, B., Jiang, F., Li, L. Li, D., Zhu, X., Pan, A.: Growth of CdSe/MoS_2 vertical heterostructures for fast visible-wavelength photodetectors. J. Alloys Compd. **815**, 152309 (2020)
10. Jeon, H.B., Shin, G.H., Lee, K.J., Choi, S.Y.: Vertical-tunneling field-effect transistor based on WSe_2-MoS_2 heterostructure with ion gel dielectric. Adv. Electron. Mater. **6**(7), 2000091 (2020).
11. Gong, Y., Lin, J., Wang, X., Shi, G., Lei, S., Lin, Z., Zou, X., Ye, G., Vajtai, R., Yakobson, B.I., Terrones, H., Terrones, M., Tay, B.K., Lou, J., Pantelides, S.T., Liu, Z., Zhou, W., Ajayan, P.M.: Vertical and in-plane heterostructures from WS_2/MoS_2 monolayers. Nat. Mater. **13**(12), 1135–1142 (2014)
12. Li, M.Y., Shi, Y., Cheng, C.C., Lu, L.S., Lin, Y.C., Tang, H.L., Tsai, M.L., Chu, C.W., Wei, K.H., He, J.H., Chang, W.H., Suenaga, K., Li, L.J.: NANOELECTRONICS. Epitaxial growth of a monolayer WSe_2-MoS_2 lateral p–n junction with an atomically sharp interface. Science **349**(6247), 524–528 (2015)
13. Li, F., Feng, Y., Li, Z., Ma, C., Qu, J., Wu, X., Li, D., Zhang, X., Yang, T., He, Y., Li, H., Hu, X., Fan, P., Chen, Y., Zheng, B., Zhu, X., Wang, X., Duan, X., Pan, A.: Rational kinetics control toward universal growth of 2D vertically stacked heterostructures. Adv. Mater. **31**(27), e1901351 (2019)
14. Yang, T., Zheng, B., Wang, Z., Xu, T., Pan, C., Zou, J., Zhang, X., Qi, Z., Liu, H., Feng, Y., Hu, W., Miao, F., Sun, L., Duan, X., Pan, A.: Van der Waals epitaxial growth and optoelectronics of large-scale WSe_2/SnS_2 vertical bilayer p–n junctions. Nat. Commun. **8**(1), 1906 (2017)
15. Wu, X., Wang, X., Li, H., Zeng, Z., Zheng, B., Zhang, D., Li, F., Zhu, X., Jiang, Y., Pan, A.: Vapor growth of WSe_2/WS_2 heterostructures with stacking dependent optical properties. Nano Res. **12**(12), 3123–3128 (2019)
16. Li, F., Xu, B., Yang, W., Qi, Z., Ma, C., Wang, Y., Zhang, X., Luo, Z., Liang, D., Li, D., Li, Z., Pan, A.: High-performance optoelectronic devices based on van der Waals vertical $MoS_2/MoSe_2$ heterostructures. Nano Res. **13**(4), 1053–1059 (2020)
17. Zhang, W., Chiu, M.H., Chen, C.H., Chen, W., Wee, A.: Role of metal contacts in high-performance phototransistors based on WSe_2 monolayers. ACS Nano **8**(8), 8653–8661 (2014)
18. Huang, Y., Deng, H.X., Xu, K., Wang, Z.X., Wang, Q.S., Wang, F.M., Wang, F., Zhan, X.Y., Li, S.S., Luo, J.W., He, J.: Highly sensitive and fast phototransistor based on large size CVD-grown SnS_2 nanosheets. Nanoscale **7**(33), 14093–14099 (2015)

19. Sanne, A., Ghosh, R., Rai, A., Yogeesh, M.N., Shin, S.H., Sharma, A., Jarvis, K., Mathew, L., Rao, R., Akinwande, D., Banerjee, S.: Radio frequency transistors and circuits based on CVD MoS_2. Nano. Lett. **15**(8), 5039–5045 (2015)
20. Kwon, H., Garg, S., Park, J.H., Jeong, Y., Yu, S., Kim, S.M., Kung, P., Im, S.: Monolayer MoS_2 field-effect transistors patterned by photolithography for active matrix pixels in organic light-emitting diodes. NPJ 2D Mater. Appl. **3**(1), 9 (2019)
21. Shidpour, R., Manteghian, M.: A density functional study of strong local magnetism creation on MoS_2 nanoribbon by sulfur vacancy. Nanoscale **2**(8), 1429–1435 (2010)
22. Komsa, H.-P., Krasheninnikov, A.V.: Effects of confinement and environment on the electronic structure and exciton binding energy of MoS_2 from first principles. Phys. Rev. B **86**(24), 241201 (2012)
23. Gong, F., Fang, H., Wang, P., Su, M., Li, Q., Ho, J.C., Chen, X., Lu, W., Liao, L., Wang, J., Hu, W.: Visible to near-infrared photodetectors based on MoS_2 vertical Schottky junctions. Nanotechnology. **28**(48), 484002 (2017)
24. Chen, Y., Wang, X., Wu, G., Wang, Z., Fang, H., Lin, T., Sun, S., Shen, H., Hu, W., Wang, J., Sun, J., Meng, X., Chu, J.: High-performance photovoltaic detector based on $MoTe_2/MoS_2$ van der Waals heterostructure. Small **14**(9), 1870038 (2018)
25. Liu, B., Tang, B., Lv, F., Zeng, Y., Liao, J., Wang, S., Chen, Q.: Photodetector based on heterostructure of two-dimensional WSe_2/In_2Se_3. Nanotechnology **31**(6), 065203 (2020)
26. Wang, P., Liu, S., Luo, W., Fang, H., Gong, F., Guo, N., Chen, Z.G., Zou, J., Huang, Y., Zhou, X., Wang, J., Chen, X., Lu, W., Xiu, F., Hu, W.: Arrayed van der Waals broadband detectors for dual-band detection. Adv. Mater. **29**(16), 1604439 (2017)
27. Li, C., Yan, X., Song, X., Bao, W., Ding, S., Zhang, D.W., Zhou, P.: WSe_2/MoS_2 and $MoTe_2/SnSe_2$ van der Waals heterostructure transistors with different band alignment. Nanotechnology **28**(41), 415201 (2017)

Yu Xiao received the B.S degree of Metal Material Engineering from Nanchang Hangkong University, China. In September 2019, she was admitted as a postgraduate in Hunan University, China and then she joined the Key Laboratory of Micro-Nano Physics and Technology for relative research.

Junyu Qu is currently a Ph.D. candidate at the College of Materials Science and Engineering in Hunan University, China. His research interests include the growth the low dimensional nanomaterials, fabrication of low dimensional van der Waals heterostructures and their applications in electronics and optoelectronics.

Ziyu Luo received the B.S. degree from the School of Electrical Engineering and Automation, Harbin Institute of Technology, China in 2014. He is now a Ph.D. candidate at the College of Materials Science and Engineering in Hunan University, China. His research interests focus on the ultrafast spectrum with time and spatial-resolved of two-dimensional transition metal dichalcogenides materials and perovskites heterojunctions.

Ying Chen is currently a Ph.D. candidate at the College of Materials Science and Engineering, Hunan University, China. His main research interests include the synthesis of nanomaterials with controlled CVD route, and their applications in photoelectric devices.

Xin Yang received his B.Sc. degree from Anhui University, China in 2014. From 2016/09, He studied at the Key Laboratory for Micro-Nano Physics and Technology of Hunan Province, Hunan University, China as a doctoral candidate. His research interests are low-dimensional semiconductor optoelectronics.

Danliang Zhang is currently a PhD candidate at the School of Physics and Electronics, Hunan University, China. His research interests focus on spin-valleytronics and nonlinear optics of two-dimensional materials. He has published 14 SCI-indexed peer-reviewed papers, including Nature Communications, Advanced Materials.

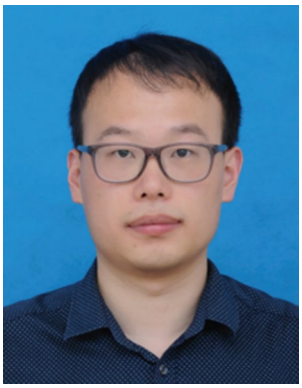

Honglai Li received his Bachelor degree in Physics, and Ph.D. degree in Condensed Matter Physics from Hunan University, China; then taught there as a Yuelu Scholar in 2017. His main research interests lie in the controlled growth of low dimensional semiconductor structures, and physical properties as well as device applications of nanostructures.

Biyuan Zheng received his B.S. degree in School of Chemistry and Chemical Engineering in 2014, and his Ph.D. degree in School of Physics and Electronics in 2020 from Hunan University, China. He is now a Postdoctoral Fellow at College of Materials Science and Engineering, Hunan University. His research interests focus on synthesis of novel 2D semiconductor nanostructures for optical and electrical applications.

Jiali Yi is currently a Ph.D. candidate at the School of Materials Science and Engineering, Hunan University, China. The main research direction is the application of two-dimensional semiconductor materials in multifunctional logic circuits.

Rong Wu a master student at the school of Materials Science and Engineering, Hunan University, China. Her main research interests is the synthesis of two-dimensional semiconductor heterojunctions by vapor deposition and their optoelectronic properties.

Wenxia You is currently a master student at the School of Materials Science and Engineering, Hunan University, China. Her main research interests include the synthesis of two-dimensional materials by controllable CVD route and their application in optoelectronic devices.

Bo Liu is currently a master student at the School of Materials Science and Engineering, Hunan University, China. His main research interests include the synthesis of nanomaterials by controllable CVD route and their application in optics.

Shula Chen received his B.Sc. degree from Fudan University, China in 2008 and Ph.D. degree from Linköping University, Sweden in 2014. From 2014 to 2016, he worked at Hokkaido University, Japan as postdoctoral researcher. After that, he returned to Linköping University as postdoctor and was later promoted to be assistant professor in 2017. In 2018, he joined College of Materials Science and Engineering at Hunan University, China as professor. His main research interests include nanooptics and ultrafast photo-physics of novel low-dimensional semiconductors and related devices based on 2D materials, Perovskites, and III-V dilute nitride semiconductors.

Anlian Pan received his Ph.D. degree from the Institute of Physics, Chinese Academy of Sciences, China in 2006. Afterwards, he worked for one year as a Humboldt Research Fellow with Prof. Ulrich Goesele at Max Planck Institute of Microstructure Physics, Germany, and then joined Arizona State University, USA as a Postdoctoral Fellow, where he became a research assistant professor. He came back to Hunan University, China in 2010 and has been working as the distinguished professor of "Furong" scholar in Hunan Province since then. His research interests include the micro-nano optical, electronics of semiconductor nanostructures.